

## **NH<sub>3</sub> Adsorption on Anatase-TiO<sub>2</sub>(101)**

Stig Koust,<sup>1</sup> Kræn Adamsen,<sup>1</sup> Esben Leonhard Kolsbjerg,<sup>1,2</sup> Zheshen Li,<sup>2</sup> Bjørk Hammer,<sup>1,2</sup> Stefan Wendt,<sup>1</sup> and Jeppe V. Lauritsen<sup>1, a)</sup>

<sup>1)</sup>*Interdisciplinary Nanoscience Center, Aarhus University, DK-8000 Aarhus C, Denmark*

<sup>2)</sup>*Department of Physics and Astronomy, Aarhus University, DK-8000 Aarhus C, Denmark*

(Dated: 4 January 2018)

The adsorption of ammonia on anatase TiO<sub>2</sub> is of fundamental importance for several catalytic applications of TiO<sub>2</sub> and for probing acid-base interactions. Utilizing high-resolution scanning tunneling microscopy (STM), synchrotron X-ray photoelectron spectroscopy (XPS), temperature-programmed desorption (TPD) and density functional theory (DFT), we identify the adsorption mode and quantify adsorption strength on the anatase TiO<sub>2</sub>(101) surface. It was found that ammonia adsorbs non-dissociatively as NH<sub>3</sub> on regular five-fold coordinated titanium surface sites (5f-Ti) with an estimated exothermic adsorption energy of 1.2 eV for an isolated ammonia molecule. For higher adsorbate coverages, the adsorption energy progressively shifts to smaller values, due to repulsive intermolecular interactions. The repulsive adsorbate-adsorbate interactions are quantified using DFT and autocorrelation analysis of STM images, which both showed a repulsive energy of ~50 meV for nearest neighbour sites and a lowering in binding energy for an ammonia molecule in a full monolayer of 0.28 eV, which is in agreement with TPD spectra.

---

<sup>a)</sup>Electronic mail: jvang@inano.au.dk

## I. INTRODUCTION

Titanium dioxide ( $\text{TiO}_2$ ) is used in many applications such as Grätzel solar cells,<sup>6</sup> heterogeneous catalysis<sup>2,7-9</sup> and photocatalysis.<sup>10,11</sup> Among the main polymorphs of  $\text{TiO}_2$ , rutile, anatase and brookite, only the former two are used in technical applications.<sup>2,11</sup> Whereas rutile has traditionally been the most studied polymorph in the surface science literature,<sup>11</sup> anatase has bulk and surface properties that makes this polymorph the most relevant for e.g. photocatalytic and heterogeneously catalysed reactions.

For this reason, the most stable of the anatase facets, the  $\text{TiO}_2(101)$  surface (a- $\text{TiO}_2(101)$ ), has been the subject of numerous studies addressing the adsorption of small molecules, such as  $\text{CO}$ ,<sup>12,13</sup>  $\text{H}_2\text{O}$ ,<sup>14-16</sup>  $\text{O}_2$ <sup>17</sup> and acetic acid.<sup>18</sup> These studies have shown a rather complex behaviour of these simple molecules, although their adsorption seems to be less dominated by bulk and surface defects than for rutile  $\text{TiO}_2$ . Here we focus on the fundamental interaction of  $\text{NH}_3$  with a- $\text{TiO}_2(101)$ . The  $\text{NH}_3$  adsorption on a- $\text{TiO}_2(101)$  is highly important, insofar as adsorption studies of  $\text{NH}_3$  with a- $\text{TiO}_2$  have been used to probe Lewis acid-base interactions with anatase powders.<sup>1</sup> In addition, the  $\text{NH}_3$ /anatase  $\text{TiO}_2$  system is of importance in the selective catalytic reduction (SCR) of  $\text{NO}$  with  $\text{NH}_3$  using submonolayer vanadium oxides on a- $\text{TiO}_2$ <sup>2,3</sup> or for titania based catalyst for removal of  $\text{NH}_3$  pollution from air and water.<sup>4,5</sup>

Studies addressing the  $\text{NH}_3$  adsorption on the rutile polymorph, r- $\text{TiO}_2(110)$ , have employed scanning tunneling microscopy (STM),<sup>19</sup> temperature programmed desorption (TPD),<sup>20,21</sup> X-ray photoemission spectroscopy (XPS)<sup>21-23</sup> and theoretical calculations<sup>1,24,25</sup> to conclude that ammonia adsorbs molecularly on five-fold coordinated titanium (5f-Ti) surface sites and desorbs again without dissociation. The desorption energy was found to be coverage-dependent and decrease from  $\sim 1.0$ - $1.3$  eV<sup>20,21</sup> at low  $\text{NH}_3$  coverage to  $\sim 0.6$  eV at full monolayer coverage. This is reasoned by repulsive  $\text{NH}_3$ - $\text{NH}_3$  interactions, which causes the ammonia to occupy every second 5f-Ti surface site.<sup>19,22,23,26</sup> On r- $\text{TiO}_2(110)$ , a full monolayer is therefore considered in some studies to be achieved by occupation of half the available 5f-Ti sites<sup>19,22</sup>. However, Kim *et al.*<sup>20</sup> reported by TPD that a full  $\text{NH}_3$  monolayer on rutile  $\text{TiO}_2$  (110) corresponds to occupation of all 5f-Ti sites.

The present study combines STM, XPS, TPD and density functional theory (DFT) to reveal the adsorption mode, intermolecular interactions and desorption of  $\text{NH}_3$  on a- $\text{TiO}_2(101)$ .

Our STM and DFT results reveal the preferential adsorption site to be on 5f-Ti surface sites of a-TiO<sub>2</sub>(101). We conclude that NH<sub>3</sub> adsorbs and desorbs molecularly based on XPS and TPD. In line with comparable studies of NH<sub>3</sub> monolayers on r-TiO<sub>2</sub>(110) we find that repulsive interactions between neighbouring NH<sub>3</sub> molecules influences binding energies, reflected by an observed intermediate (2×1) superstructure. However a full NH<sub>3</sub> monolayer is considered as occupation of all 5f-Ti-sites.

## II. EXPERIMENTAL

The STM and TPD experiments were performed in an Ultra-High Vacuum chamber (SPECS) with a base pressure below  $1 \times 10^{-10}$  mbar, equipped with an commercial Aarhus-type STM (Aarhus-150, SPECS) that allows for cooling to liquid nitrogen temperatures. Tungsten (W) STM tips prepared by electrochemical etching was used for imaging. Typical scanning parameters were 1000-1400 mV and 0.1-0.2 nA. All TPD spectra were acquired using a quadrapole mass spectrometer (HIDEN). The XPS experiments were carried out at the ASTRID2 synchrotron source at Institute for Storage Ring Facilities (ISA) at Aarhus University on the AU-MatLine beamline.<sup>27</sup> The beamline is equipped with a SX-700 monochromator and SCIENTA SES200 electron energy analyzer running with a pass energy of 75 eV, curved analyzer slit of 0.8 mm and a beamline monochromator slit width of 60  $\mu$ m. The base pressure was around  $5 \times 10^{-10}$  mbar. The N1s core level was collected using a photon energy of 480 eV.

Natural anatase single crystals (SurfaceNet) were prepared by preparation cycles of sputtering (Ar<sup>+</sup>, 1.5 kV,  $5 \times 10^{-7}$  mbar, 298 K), O<sub>2</sub> annealing ( $1 \times 10^{-8}$  mbar, 820-950 K) and subsequent sputtering and vacuum-annealing (820-950 K). The temperature of the sample is measured by a K-type thermocouple spot-welded onto the sample holder close to the sample. NH<sub>3</sub> was dosed on to the anatase TiO<sub>2</sub>(101) surface through a leak valve by means of a directional doser. This was done to minimize ammonia contaminants in the residual gas and thereby minimizing re-adsorption onto the surface after the initial exposure. Typical exposures for submonolayer coverage of NH<sub>3</sub> was  $5 \times 10^{-10}$  mbar for 1-2 seconds. The coverage is given in ML, with 1 ML defined as one NH<sub>3</sub> molecule per Ti surface atom in the a-TiO<sub>2</sub>(101) surface, i.e.  $9.7 \times 10^{14}$  NH<sub>3</sub> molecules per cm<sup>2</sup>.

For constructing, manipulating, and optimizing the atomistic systems the ASE<sup>28</sup> package

was used in combination the GPAW<sup>29</sup> density functional theory (DFT) code. We use the grid based mode of GPAW with a spacing of at least 0.1771 sampling  $4 \times 4 \times 1$  K-points of the Brillouin zone. To mimic the experimental crystal, we employ a 4 layer TiO<sub>2</sub> (101) anatase slab spanning  $1 \times 2$  surface unit cells resulting in a total stoichiometry of Ti<sub>24</sub>O<sub>48</sub>. We use the optB88-vdW functional with optimized lattice parameters of  $a = b = 3.82 \text{ \AA}$  and  $c = 9.61 \text{ \AA}$  with periodic boundary conditions parallel to the slab surface with at least 6  $\text{\AA}$  of vacuum from any atom to the non-periodic cell boundaries. The bottom layer was held frozen and systems were considered converged when no force on any atom exceeded 0.025 eV/ $\text{\AA}$ .

### III. RESULTS AND DISCUSSION

Figure 1 shows STM images following NH<sub>3</sub> exposure at room temperature (RT). The a-TiO<sub>2</sub>(101) surface exhibits large trapezoidal islands separated by monoatomic steps typical for this surface.<sup>30</sup> As we expose the clean a-TiO<sub>2</sub>(101) surface to 0.05 ML ammonia, bright protrusions appear in the STM image reflecting adsorption at room temperature. The ammonia-related protrusions reside homogeneously across the terraces (figure 1a). The protrusions appear to have little affinity for binding at step edges and no apparent agglomeration of molecules was observed. In order to illustrate local structural information of the adsorbed ammonia we present a high-resolution ( $6 \text{ nm} \times 6 \text{ nm}$ ) STM image in figure 1b. The superimposed lattice points (red circles) are attributed to protruding two-fold coordinated O atoms (2f-O) on a-TiO<sub>2</sub>(101). The bright features associated with ammonia (blue circles) are observed to bind in between the surface lattice rows running in the [010] direction in a position which is slightly displaced towards one of the rows. The fivefold coordinated Ti atoms (5f-Ti) terminating the a-TiO<sub>2</sub>(101) surface (grey) are also illustrated in the STM image and their position coincides with the adsorption site of ammonia. Thus, the STM data suggests that ammonia binds to the a-TiO<sub>2</sub>(101) surface on top of the 5f-Ti surface sites. In agreement we find from DFT that ammonia is predicted to adsorb molecularly without dissociation with an exothermic adsorption energy of 1.20 eV. The DFT calculated adsorption site of isolated NH<sub>3</sub> molecules on a stoichiometric a-TiO<sub>2</sub>(101) is indeed found to be on 5f-Ti, as illustrated in figure 1c. The ammonia is found off-centered between 2f-O rows running in the [010] direction.

XPS data were collected in order to verify the non-dissociative binding of molecular ammonia to a-TiO<sub>2</sub>(101). XPS allows for easy distinction between various amines as the shift in binding energy between NH<sub>2</sub>, NH<sub>3</sub> and NH<sub>4</sub> is in the order of 1.5 eV.<sup>31</sup> We exposed the a-TiO<sub>2</sub> (101) surface to more than a monolayer of ammonia at 118K and collected the N1s core level spectra (figure 2). This was followed by stepwise heating at elevated temperatures for 5 minutes until the N1s signal vanished. The XPS data were collected at ~120 K throughout the series. The N1s peak position is found at 400.9 eV for all temperatures and can be fitted with a single peak with FWHM of 1.8 eV, indicating that only a single nitrogen species is present on the surface at all temperatures. This binding energy for nitrogen corresponds to molecularly adsorbed NH<sub>3</sub> bound to a Lewis acid center, thus a NH<sub>3</sub>-Ti bond.<sup>21,22,31,32</sup> A dative bond with a Lewis acid center is formed by donation of a free electron pair from nitrogen.<sup>31</sup> The N1s intensity decreases upon heating to 147 K and further at 176 K, but then stays constant up to 273 K. Complete desorption of NH<sub>3</sub> was found after heating up to 373 K. This evolution of the N1s intensity suggest that multilayers of NH<sub>3</sub> accommodate the surface at the lowest temperature. The multilayer desorbs for temperatures around 176 K, where a stable monolayer is left on the surface, which is stable up to temperatures at 373 K. This is corroborated by TPD studies of ammonia desorption, which furthermore indicates considerable adsorbate-adsorbate interactions. In the TPD experiment, NH<sub>3</sub> was adsorbed on the a-TiO<sub>2</sub> (101) surface at ~100 K in various coverages, followed by a linear temperature ramp rate ( $\beta$ ) of 0.5 Ks<sup>-1</sup> to 600 K. The corresponding desorption spectra ( $m/z = 17$ ) are presented in figure 3. The coverage is estimated by relating the integrated areas for the different spectra to the spectrum where multilayers start forming. At the lowest coverage a single high temperature desorption peak around 410 K is observed. For higher coverages the leading edge shifts progressively towards lower temperature, whereas the trailing edge stays constant, resulting in a broadening of the desorption peak. The desorption peak maximum shifts from 410 K(lowest coverage) to 327 K(full monolayer) in the submonolayer regime. For coverages above a monolayer we observe a multi-layer desorption peak forming around 180 K. The decrease in temperature of desorption peak maximum ( $T_m$ ) for increasing NH<sub>3</sub> coverage indicates a strong coverage-dependent desorption energy ( $E_d$ ), which can be calculated on the basis of  $T_m$ . We note that this method is valid strictly for first-order desorption.<sup>33</sup> This is fulfilled for non-dissociative adsorption,<sup>20</sup> despite the shift of maximum desorption to lower temperature with increasing coverages, which is otherwise typically related to second-order

desorption.<sup>34</sup>  $E_d$  is calculated iteratively from the following equation:

$$E_d = k_b T_m \ln \left[ \frac{k_b T_m^2 \nu}{E_d \beta} \right] \quad (1)$$

where the pre-exponential factor ( $\nu$ ) is calculated as in Ref. [34] to be  $1.8 \times 10^{13} s^{-1}$ , which coincides with previously published values.<sup>20,33,34</sup>  $E_d$  as a function of coverage in the sub-monolayer regime is presented in the inset in figure 3. We observed a shift from 1.18 eV to 0.93 eV for increasing coverage. Extrapolating to the zero coverage limit yields  $E_d$  of a single ammonia molecule on a-TiO<sub>2</sub>(101) to be  $1.23 \pm 0.1$  eV, which is in excellent agreement with theory (1.2 eV). In this limit NH<sub>3</sub>-NH<sub>3</sub> interactions can be neglected; thus only the NH<sub>3</sub>-TiO<sub>2</sub> interaction is determining  $E_d$  for an isolated NH<sub>3</sub> molecule.

The TPD spectra are also in accordance with the desorption trend observed in the XPS spectra (figure 2), as multilayer coverages were seen to desorb in the temperature range below 176 K, whereas a complete desorption occurred at temperatures higher than 276 K. The strong coverage-dependent desorption energy is attributed to the repulsion between ammonia molecules.<sup>20,21</sup> A small tail is seen at the trailing edge at around 450 K, this is presumably caused by ammonia adsorption in vicinity of defects (subsurface donors), as only small affinity for adsorption at step edges is observed.

The repulsive interaction between NH<sub>3</sub> molecules was further quantified by analysing the autocorrelation function of the ammonia positions (figure 4) from our STM data (figure 5) and comparing with DFT values for adsorption with a second NH<sub>3</sub> molecule within the supercell modeling the a-TiO<sub>2</sub>(101) surface. By marking the positions of adsorbed NH<sub>3</sub> molecules in an automated process and assigning them to an adsorption site, the probabilities of occupations are calculated. This is visualized in the figure 4, by the grey scale colourmap. The experimental repulsion energy ( $E_{rep}$ ) is extracted by:<sup>12</sup>

$$E_{rep} = -kT \ln \left( \frac{p_n}{p_{av}} \right) \quad (2)$$

where  $p_n$  denotes the probability for occupying neighbouring site obtained directly from our autocorrelation analysis and  $p_{av}$  the average probability for a random 5f-Ti site (coverage). Assuming the occupation of sites follow a Boltzmann distribution the repulsion energy can be extracted. The experimentally extracted repulsion energies are displayed in figure 4 in white, on a grid reflecting the lattice of NH<sub>3</sub> adsorption sites. The values are shown together with the change in theoretical (DFT) adsorption energy with NH<sub>3</sub> the on neighbouring sites in

green. Very good agreement between theory and experimental acquired values are observed. In general, the nearest neighbour sites along the [010] are considerably less favourable than next-nearest neighbour adsorption sites and other sites further away. The nearest neighbour sites show repulsion energies of  $\sim 50$  meV, next-nearest neighbour sites show  $\sim 20$  meV and sites further away show repulsion energy close to zero which reflects randomly distributed molecules. These results are also in good qualitative agreement with the observed  $\text{NH}_3$  positions observed in figure 5 as nearest neighbour adsorption sites are rarely observed. By increasing the ammonia coverage (figure 5) the STM images show local patterns of double lattice distance along the [010] directions (figure 5). Patterns along [111] direction are also observed (figure 5). We found that at even higher coverages STM imaging becomes troublesome at room temperature, because of rapidly diffusing ammonia molecules. This can be circumvented at lower imaging temperatures ( $\sim 100$  K), where a static ordered overlayer structure can be imaged (figure 6). The overlayer consist of patches of adsorbed ammonia separated by  $\sim 5.5$  Å formed in the [111] direction upon dosage and a longer distance of 7.8 Å along [010] directions. The intermolecular distances in the ordered areas ( $7.8$  Å  $\times$   $5.6$  Å) coincides with a  $(2\times 1)$  symmetry with the underlying 5f-Ti surface atoms, i.e. a  $\text{NH}_3$ - $(2\times 1)$ - $\text{TiO}_2$  overlayer. No STM images were obtained when further increasing the  $\text{NH}_3$  coverage, thus only TPD and XPS measurement are present for full monolayer coverages.

By adding all the obtained experimental or theoretical repulsion energies (figure 4), the adsorption energy per ammonia molecule for a full monolayer (all 5f-Ti sites occupied) is estimated to be 0.28 eV less than for the low coverage situation. The shift in energy between the low coverage adsorption and a full monolayer is in agreement with desorption features in the TPD, where a shift of 0.28 eV is seen figure 3, insert i.e.  $\text{NH}_3$  in a full monolayer is destabilized by this energy compared to a single  $\text{NH}_3$ . Compared with the  $\text{NH}_3$ /rutile- $\text{TiO}_2(110)$  system<sup>20,21</sup> the adsorption of  $\text{NH}_3$  on  $\text{TiO}_2(101)$  is very similar. The  $\text{NH}_3$  adsorption sites is on 5f-Ti atoms on both surfaces. For a- $\text{TiO}_2(101)$  we detect a significant  $\text{NH}_3$ - $\text{NH}_3$  repulsion reflected by a coverage-dependent desorption energy, but the effect is weaker than on rutile- $\text{TiO}_2(110)$ , which can be explained by a larger 5f-Ti spacing in anatase (101) compared to rutile (110)  $\text{TiO}_2$  (3.78 Å and 2.96 Å respectively).

## IV. CONCLUSION

In summary, by high-resolution STM combined with XPS, TPD and DFT, we find that  $\text{NH}_3$  adsorbs molecularly on anatase  $\text{TiO}_2$  (101). Specifically, when  $\text{NH}_3$  was deposited at sub-monolayer coverage at room temperature, we found an affinity for  $\text{NH}_3$  to reside at 5f-Ti atom sites. The theoretical adsorption energy(DFT) was calculated to be 1.20 eV and measured by TPD analysis to be 1.23 eV. Our XPS and TPD data indicated that  $\text{NH}_3$  did not undergo dissociation at elevated temperature and desorped molecularly. Upon increasing the coverage, the  $\text{NH}_3$  adsorption energy was significantly lowered by 0.28 eV because of dipole-dipole repulsive interactions, confirmed by TPD and autocorrelation analysis of STM images. In addition, the strong interaction between  $\text{NH}_3$  resulted in a preference for occupying next-nearest 5f-Ti neighbour sites along the [010] direction, whereas  $\text{NH}_3$  molecules occupying adjacent nearest neighbour sites in the [101] direction was seldom and an repulsion energy of  $\sim 50$  meV was found for this site from DFT and autocorrelation analysis of low  $\text{NH}_3$  coverage STM images. Furthermore, an intermediate ( $2\times 1$ ) overlay  $\text{NH}_3$  adsorbate structure was observed at low temperature as a result of the intermolecular interaction.

## ACKNOWLEDGMENTS

This work was partly funded by the Innovation Fund Denmark (IFD) under File No. 12-132681 (Cat-C), File No. 6151-00008B (ProNOx), VILLUM FONDEN (Investigator grant, project number 16562), and Danish Research Councils (0602-02566B). We gratefully acknowledge support from Haldor Topsøe A/S. We acknowledge beamtime received at ASTRID2 on the MatLine beamline

## REFERENCES

- <sup>1</sup>A. Markovits, J. Ahdjoudj, and C. Minot. *Surf. Sci.*, **365**, 649 (1996).
- <sup>2</sup>G. Busca, L. Lietti, G. Ramis, and F. Berti. *Appl. Catal. B*, **18**, 1 (1998).
- <sup>3</sup>I. E. Wachs, G. Deo, B. M. Weckhuysen, A. Andreini, M. Vuurman, M. de Boer, and M. D. Amiridis. *J. Cat.*, **221**, 211 (1996).
- <sup>4</sup>J. Lee, H. Park, and W. Choi. *Environ. Sci. Technol.*, **36**, 5462 (2002).



- <sup>5</sup>S. Yamazoe, T. Okumura, Y. Hitomi, T. Shishido, and T. Tanaka. *J. Phys. Chem. C*, **111**, 11077 (2007).
- <sup>6</sup>M. Grätzel. *J. Photochem. Photobiol. C*, **4**, 145 (2003).
- <sup>7</sup>I. E. Wachs. *Dalton Trans.*, **42**, 11762 (2013).
- <sup>8</sup>L. Artiglia, S. Agnoli, and G. Granozzi. *Coord. Chem. Rev.*, **301**, 106 (2015).
- <sup>9</sup>N. Y. Topsøe, H. Topsøe, and J. Dumesic. *J. Catal.*, **151**, 226 (1995).
- <sup>10</sup>B. M. Weckhuysen and D. E. Keller. *Catal. Today*, **78**, 25 (2003).
- <sup>11</sup>U. Diebold. *Surf. Sci. Rep.*, **48**, 53 (2003).
- <sup>12</sup>M. Setvin, M. Buchholz, W. Hou, C. Zhang, B. Stöger, J. Hulva, T. Simschitz, X. Shi, J. Pavelec, G. S. Parkinson, M. Xu, Y. Wang, M. Schmid, C. Wöll, A. Selloni, and U. Diebold. *J. Phys. Chem. C*, **119**, 21044 (2015).
- <sup>13</sup>M. Setvin, B. Daniel, U. Aschauer, W. Hou, Y-F. Li, M. Schmid, A. Selloni, and U. Diebold. *Phys. Chem. Chem. Phys.*, **16**, 21524 (2014).
- <sup>14</sup>C. Dette, M. A. Pérez-Osorio, S. Mangel, F. Giustino, S. J. Jung, and K. Kern. *J. Phys. Chem. C*, **121**, 1182 (2017).
- <sup>15</sup>Y. He, A. Tilocca, O. Dulub, A. Selloni, and U. Diebold. *Nat. Mater.*, **8**, 585 (2009).
- <sup>16</sup>G. S. Herman, Z. Dohnalek, N. Ruzycski, and U. Diebold. *J. Phys. Chem. B*, **107**, 2788 (2003).
- <sup>17</sup>M. Setvín, M. Wagner, M. Schmid, G. S. Parkinsona, and U. Diebold. *Chem. Soc. Rev.*, **46**, 1772 (2017).
- <sup>18</sup>D. C. Grinter, M. Nicotra, and G. Thornton. *J. Phys. Chem. C*, **116**, 11643 (2012).
- <sup>19</sup>C. L. Pang, A. Sasahara, and H. Onishi. *Nanotechnol.*, **18**, 44003, (2007).
- <sup>20</sup>B. Kim, Z. Li, B. D. Kay, Z. Dohnalek, and Y. K. Kim. *Phys. Chem. Chem. Phys.*, **14**, 15060 (2012).
- <sup>21</sup>E. Farfan-Arribas and R. J. Madix. *J. Phys. Chem. B*, **107**, 3225 (2003).
- <sup>22</sup>U. Diebold and T.E. Madey. *J. Vac. Sci. Technol. A*, **10**, 2327 (1992).
- <sup>23</sup>W. K. Siu, R. A. Bartynski, and S. L. Hulbert. *J. Chem. Phys.*, **113**, 10697 (2000).
- <sup>24</sup>D. Cheng, J. Lan, D. Cao, and W. Wang. *Appl. Catal. B*, **106**, 510 (2011).
- <sup>25</sup>J. G. Chang, S. P. Ju, C. S. Chang, and H. T. Chen. *J. Phys. Chem. C*, **113**, 6663 (2009).
- <sup>26</sup>J. N. Wilson and H. Idriss. *Langmuir*, **20**, 10956 (2004).
- <sup>27</sup>Zheshen Li. <http://www.isa.au.dk/facilities/astrid2/beamlines/AU-Matline/AU-Matline.asp>.

- <sup>28</sup>A. Larsen, J. Mortensen, J. Blomqvist, I. Castelli, R. Christensen, M. Dulak, J. Friis, M. Groves, B. Hammer, C. Hargus, E. Hermes, P. Jennings, P. B. Jensen, J. Kermode, J. Kitchin, E. L. Kolsbjerg, J. Kubal, K. Kaasbjerg, S. Lysgaard, J. B. Maronsson, T. Maxson, T. Olsen, L. Pastewka, A. Peterson, C. Rostgaard, J. Schiøtz, O. Schütt, M. Strange, K. S. Thygesen, T. Vegge, L. Wilhelmson, M. Walter, Z. Zeng, and K. W. Jacobsen. *J. Phys. Condens. Matt.*, **29**, 273002 (2017).
- <sup>29</sup>J. Enkovaara, C. Rostgaard, J. J. Mortensen, J. Chen, M. Dulak, L. Ferrighi, J. Gavnholt, C. Glinsvad, V. Haikola, H. A. Hansen, H. H. Kristoffersen, M. Kuisma, A. H. Larsen, L. Lehtovaara, M. Ljungberg, O. Lopez-Acevedo, P. G. Moses, J. Ojanen, T. Olsen, V. Petzold, N. A. Romero, J. Stausholm-Møller, M. Strange, G. A. Tritsarlis, M. Vanin, M. Walter, B. Hammer, H. Häkkinen, G. K. H. Madsen, R. M. Nieminen, J. K. Nørskov, M. Puska, T. T. Rantala, J. Schiøtz, K. S. Thygesen, and K. W. Jacobsen. *J. Phys. Condens. Matt.*, **22**, 253202 (2010).
- <sup>30</sup>W. Hebenstreit, N. Ruzycki, G. S. Herman, Y. Gao, and U. Diebold. *Phys. Rev. B*, **62**, R16334 (2000).
- <sup>31</sup>C. Guimon, A. Gervasini, and A. Auroux. *J. Phys. Chem. B*, **105**, 10316 (2001).
- <sup>32</sup>J. Keränen, C. Guimon, E. Iiskola, A. Auroux, and L. Niinistö. *Catal. Today*, **78**, 149 (2003).
- <sup>33</sup>A. M. de Jong and J. W. Niemantsverdriet. *Surf. Sci.*, **233**, 355 (1990).
- <sup>34</sup>I. Chorkendorff and J. W. Niemantsverdriet. *Concepts of Modern Catalysis and Kinetics* (Wiley, 2003).

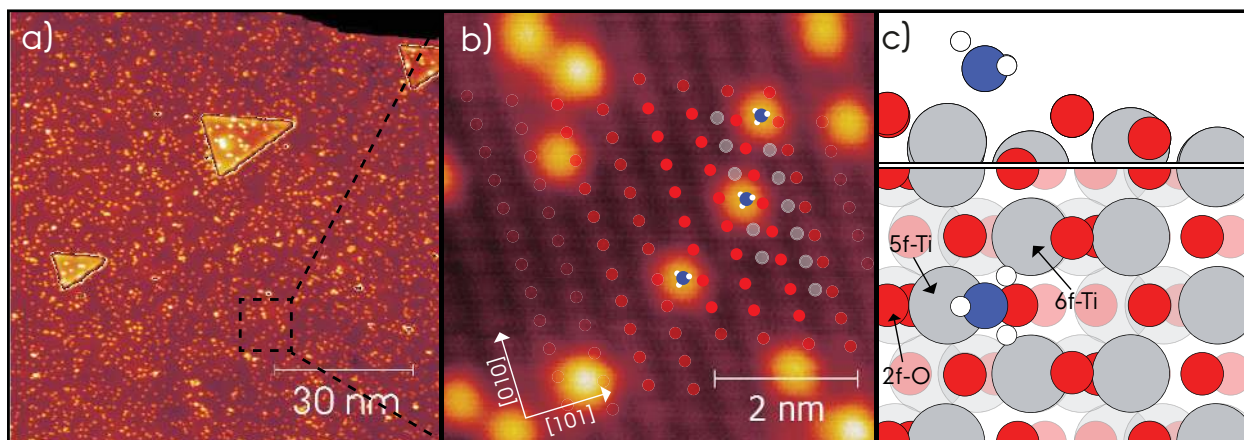


FIG. 1. a) STM image ( $120 \text{ nm} \times 120 \text{ nm}$ ) of  $0.05 \text{ ML NH}_3$  adsorbed on anatase- $\text{TiO}_2(101)$  imaged at RT. b) Atom-resolved STM ( $6 \text{ nm} \times 6 \text{ nm}$ ) image showing the  $\text{NH}_3$  adsorption site. Rows of surface lattice points (2f-O (red) and 5f-Ti(grey)) are superimposed.  $\text{NH}_3$  (blue/white) molecules resides between rows, on top of the 5f-Ti sublattice. c) DFT predicted  $\text{NH}_3$  adsorption site on 5f-Ti.

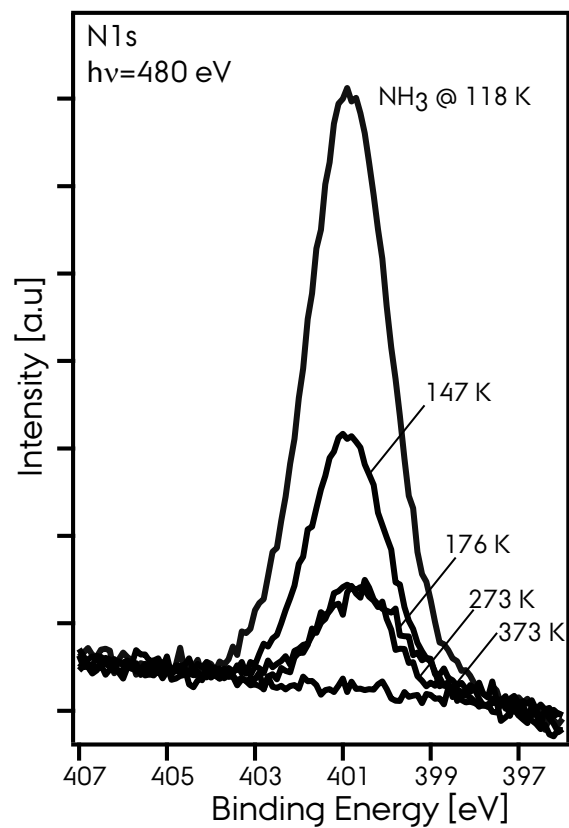


FIG. 2. N1s XPS spectra ( $h\nu = 480$  eV, data collection at 110 K) of  $\text{NH}_3$  adsorbed on anatase  $\text{TiO}_2$  (101) (at 110K) after heating in the range 118 K to 373 K.

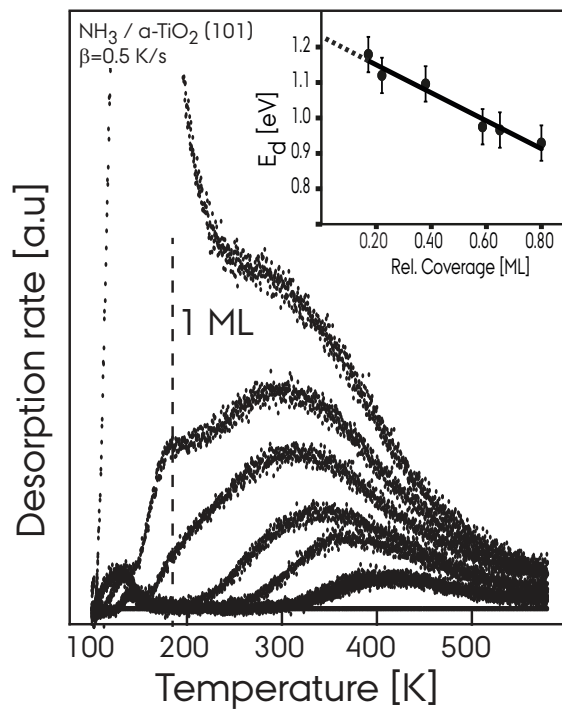


FIG. 3. TPD spectra of NH<sub>3</sub> ( $m/z = 17$ ) adsorbed on anatase-TiO<sub>2</sub>(101) for various coverages (0.2 to 1.8 ML). Insert shown redhead analysis of TPD spectra i.e. showing the change in binding energy as function of coverage (peak area).

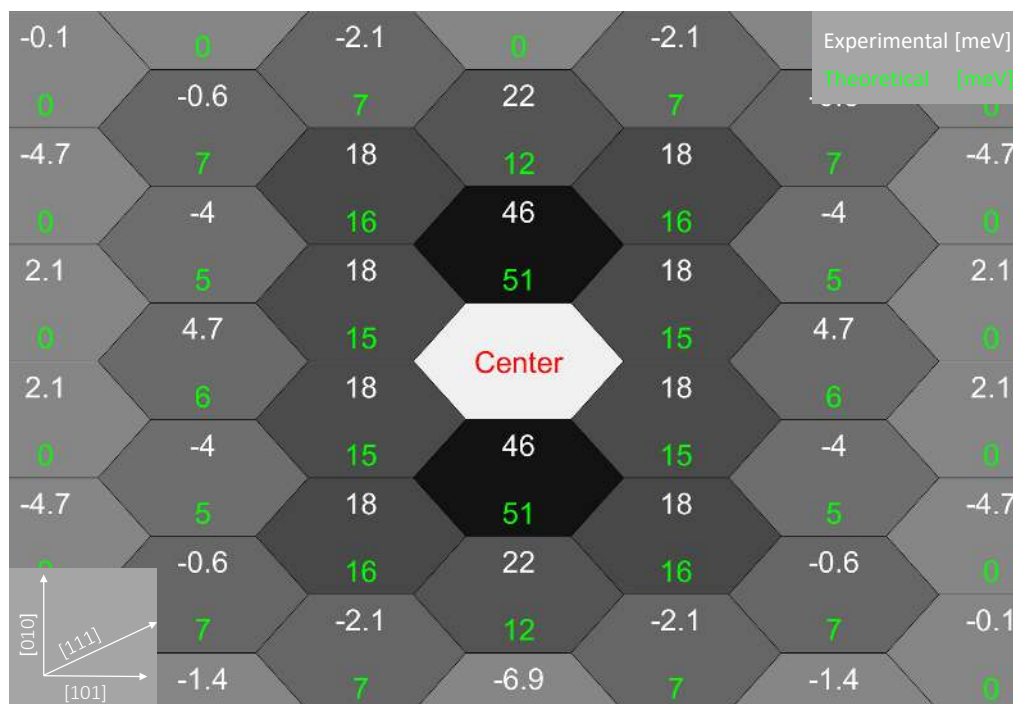


FIG. 4. Result of the autocorrelation function analysis, showing the obtained repulsion energies. Experimental in white and theoretical in green. Each hexagon represents a neighbouring Ti-5f site to the center. The grey colour scale of each tile represents its likelihood of occupation ( $p_n$ ). Black: less probable i.e. high repulsion energy, white: very probable, grey: no effect.

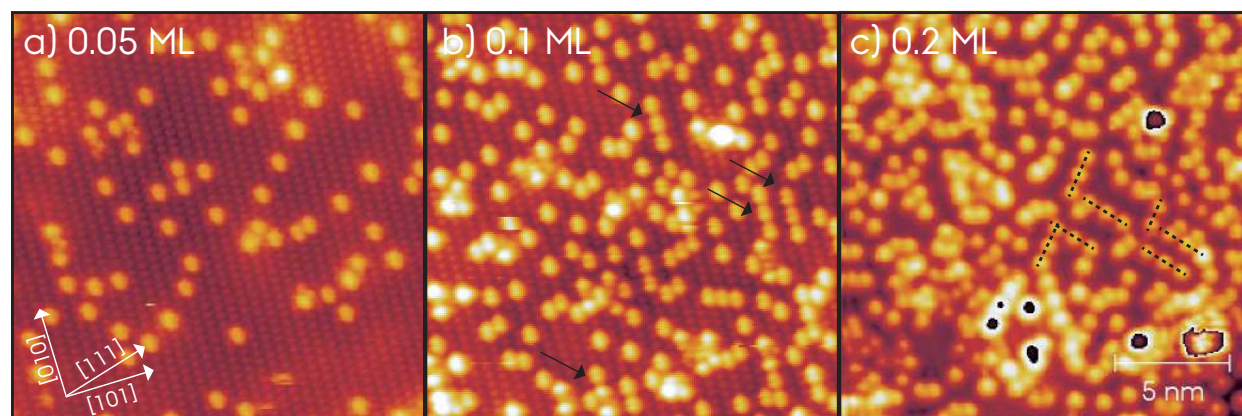


FIG. 5. STM ( $18 \text{ nm} \times 18 \text{ nm}$ ) image of  $\text{NH}_3$  adsorbed on anatase- $\text{TiO}_2(101)$  at RT at various coverages. a) 0.05 ML, b) 0.1 ML, c) 0.2 ML.

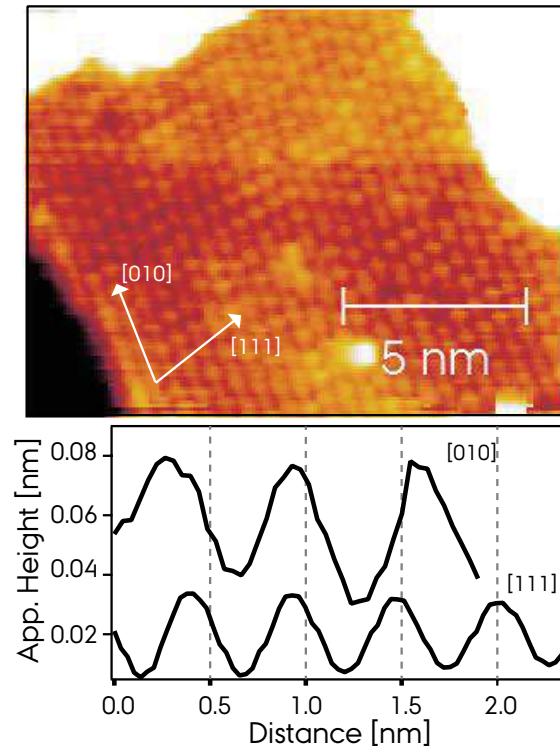


FIG. 6. STM ( $15 \text{ nm} \times 11 \text{ nm}$ ) image of  $\text{NH}_3$  adsorbed on anatase- $\text{TiO}_2(101)$  at 110 K. Inset: Linescan along the [111] and [010] directions, respectively.